June 2024

A study of radiative corrections to the mass spectrum in the Scale Invariant Two Higgs Doublet Model with an additional Real Singlet

Noah Ben Moussa

Theoretical Particle Physics
Division of Particle and Nuclear Physics
Department of Physics
Lund University

Bachelor thesis supervised by Roman Pasechnik

LUND
UNIVERSITY

Abstract

In this thesis, we study the Higgs boson mass spectrum of a Scale Invariant Two Higgs Doublet Model that includes an additional real singlet. This model results in three neutral CP-even states due to the mixing with the singlet. At tree level, one of these states has zero mass. To obtain a consistent and accurate mass spectrum for the Higgs bosons, the scale invariance is broken by incorporating radiative 1-loop corrections into the model as well as a renormalization scale.

Populärvetenskaplig beskrivning

Standardmodellen inom partikelfysik har besvarat många av de frågor som människan har ställt genom åren. Till exempel har vi fått svar på frågor som: Vad är de minsta partiklarna uppbyggda av? Vilka krafter får dem att röra sig som de gör? Hur får partiklar sin massa? Även om många frågor har fått svar, leder varje öppnad dörr till en ny dörr bakom, med ett nytt lås vars nyckel ännu inte har hittats. Det finns många frågor kvar att utforska, vilket leder oss till att tro att Standardmodellen inte är den slutgiltiga modellen och att det finns ytterligare svar att upptäcka.

Modellen som diskuteras i denna uppsats kallas för Skalinvariant Två-Higgsdublettmodellen med en tillagd reell singlet (SI-2HDM+S). Den utvidgar Standardmodellen genom att lägga till en extra Higgsdublett och en reell singlet. I denna modell inkluderas inte massor i potentialens ekvation från början, vilket innebär att dessa partikelmassor inte antas vara ursprungliga egenskaper. Modellen innehåller totalt nio olika fält som används för att bestämma partiklarnas massor. Dessa massor bestäms genom spontant symmetribrott och kvantmekaniska korrektioner, vilket är avgörande för att återskapa de massvärden vi observerar. Det intressanta med denna modell är den tillagda singleten, som öppnar nya perspektiv på symmetribrott och bidrar till att hitta möjliga lösningar på vissa av Standardmodellens begränsningar.

I detta projekt används datorbaserade simuleringar för att utforska hur olika parametrar påverkar modellens resultat. Kritiska parametrar, såsom Higgsfältens vakuumvärden, kopplingskonstanter och massor för de skalära fälten, identifieras för att bestämma vilka som har störst inverkan på partikelmassorna och symmetribrott, vilket är essentiellt för framtida experimentella studier. Med hjälp av ett datorprogram kan ett brett spektrum av scenarier noggrant undersökas, vilket möjliggör en detaljerad kartläggning av de mest relevanta parametrarna. Denna metod är avgörande för att förstå vilka faktorer som påverkar modellens förutsägelser och för att optimera experimentella strategier i jakten på nya fysikaliska fenomen.

Contents

1 Introduction

The Standard Model (SM) of particle physics [1] has been constructed by integrating multiple theories [2], each contributing a crucial piece of understanding regarding the actions of particles and their properties. A notable moment was when Peter Higgs and François Englert were awarded the Nobel Prize in 2013 for their theory on how particles acquire mass, which had been experimentally confirmed a year earlier at CERN by the CMS and ATLAS experiments [3]. Higgs' theory applies the concept of spontaneous symmetry breaking (SSB) to the symmetrical structure of the Lagrangian, the mathematical framework used to model the dynamics of fields and particles. Specifically, a structure known as the SU(2) Higgs doublet, denoted H, is introduced [4]. This doublet is essential for initiating Electroweak Symmetry Breaking (EWSB) [5], a process vital for enabling particles such as the $W^{\pm}$ and Z bosons, as well as fermions, to gain mass through the Higgs mechanism [6].

Despite these advancements, significant questions such as baryon asymmetry [7] and the nature of dark matter [8] remain, necessitating further enhancements to the SM. The Two Higgs Doublet Model (2HDM) extends the SM by introducing an additional Higgs doublet [9], facilitating a richer scalar sector which provides a framework for exploring additional scenarios that can be tested through particle collider experiments. This model has been further extended with multiple variations [10], one of which will be analyzed in this paper.

The model analyzed is a scale invariant 2 Higgs Doublet Model plus an additional real singlet (SI-2HDM+S), and it largely follows the steps outlined by Lee & Pilaftsis in their paper on SI-2HDM [11]. Through the Coleman-Weinberg (CW) mechanism [12], quantum loop corrections introduce logarithmic terms to the potential. These radiative corrections provide the necessary conditions for EWSB [4], where the vacuum expectation values (vevs) of the scalar fields are generated. This method offers a natural solution to the hierarchy problem by stabilizing the Higgs boson's mass against large quantum corrections, thus providing a more fundamental understanding of the mass generation mechanisms in particle physics. Additionally, the Gildener-Weinberg (GW) renormalization scheme [13] will be followed to ensure that the theoretical predictions are finite and match experimental results. Furthermore, $\mathbb{Z}_2$ symmetry will be imposed on the Higgs doublets to remove flavor-changing neutral currents (FCNC). Finally, exploration of the parameter space within the SI-2HDM+S is performed to identify the model's constraints and pinpoint the conditions under which new phenomena may emerge.

This thesis is structured as follows: Section 2, comprised of smaller subsections, first presents the foundational knowledge of the Higgs doublets and the 2HDM model. It then introduces the SI-2HDM+S model, explores its potential, and analyzes its mass spectrum. The section concludes by examining the 1-loop radiative corrections, utilizing similar steps as earlier sections to analyze their first derivative and tadpole conditions. Section 3 outlines the necessary steps for conducting a numerical analysis of the model. Section 4 presents the results and includes a comprehensive discussion. Finally, the thesis concludes with a summary and an outlook for potential future research.

2 Theoretical Background

2.1 Higgs Sector

Before delving into the specifics of the 2HDM+S model, it is important to establish a fundamental understanding of the structure and theory of the Higgs sector within the general theoretical context, which is the focus of this section.

The 2HDM Langrangian possesses a $SU(2)_L \times U(1)_Y$ symmetry [4] which breaks under EWSB into $U(1)_{EM}$ symmetry and contains two scalar doublets, with hypercharge Y = +1, in the scalar potential:

$$H_i = \begin{pmatrix} \phi_i^+ \\ \frac{1}{\sqrt{2}}(v_i + \varphi_i^0 + i a_i^0) \end{pmatrix}, \quad \text{with} \quad i = 1, 2. \tag{2.1}$$

A total of 8 different fields are represented, each doublet contributing a charged scalar field ϕ_i^+, a neutral scalar field φ_i^0, and a neutral pseudoscalar field a_i^0 [14]. Among these, 5 are physical fields and 3 serve as Goldstone modes [15]. These fields form the basis upon which the physical mass terms are constructed. The doublets are expanded around their respective vevs, obtained via EWSB, and can be defined as:

$$\langle H_i \rangle = \frac{v_i}{\sqrt{2}} \begin{pmatrix} 0 \\ 1 \end{pmatrix}, \quad i = 1, 2. \tag{2.2}$$

The vevs, denoted by v_1 and v_2, play a critical role in the mass generation mechanisms of the model. The EW scale parameter v, defined as $v = \sqrt{\sum_i v_i^2}$ in the Higgs sector, must be approximately 246 GeV [16] to match the mass scale of $W^\pm$, Z^0 gauge bosons. The vevs v_1 and v_2 are denoted by $v_1 \equiv v \cos\beta = v c_\beta$ and $v_2 \equiv v \sin\beta = v s_\beta$.

Additionally, the ratio of the two vevs, denoted as $\tan\beta = \frac{v_2}{v_1}$ [17] influences the coupling strengths of the Higgs bosons to fermions and gauge bosons, with the assumption of $\mathbb{Z}_2$ symmetry being explained in a subsequent section.

2.2 Scale Invariant 2HDM+S potential

Following the work of Arhrib et al, [18] we extend the model with a real singlet with hypercharge Y=0 :

$$S = \frac{1}{\sqrt{2}} \left(v_s + \varphi_s \right), \quad \text{with} \quad \langle S \rangle = \frac{1}{\sqrt{2}} v_s \tag{2.3}$$

By starting from a generic basis the potential at tree level for a 2HDM with an additional singlet (2HDM+S), similar to [18], is given as:

$$
\begin{aligned}
V_{tree}^{generic} = & m_{11}^2 H_1^\dagger H_1 + m_{22}^2 H_2^\dagger H_2 - \mu^2 \left(H_1^\dagger H_2 + H_2^\dagger H_1 \right) + \frac{1}{2} m_s^2 S^2 + \frac{\lambda_1}{2} \left(H_1^\dagger H_1 \right)^2 \\
& + \frac{\lambda_2}{2} \left(H_2^\dagger H_2 \right)^2 + \lambda_3 \left(H_1^\dagger H_1 \right) \left(H_2^\dagger H_2 \right) + \lambda_4 \left(H_1^\dagger H_2 \right) \left(H_2^\dagger H_1 \right) \\
& + \frac{\lambda_5}{2} \left[\left(H_1^\dagger H_2 \right)^2 + \left(H_2^\dagger H_1 \right)^2 \right] + \frac{\lambda_6}{8} S^4 + \frac{1}{2} \left[\lambda_7 H_1^\dagger H_1 + \lambda_8 H_2^\dagger H_2 \right] S^2 \\
& + \kappa S^3 + \xi S (H_1^\dagger H_1 + H_2^\dagger H_2) + \zeta' S (H_1^\dagger H_2 + H_2^\dagger H_1).
\end{aligned}
\tag{2.4}
$$

We have the quadratic mass terms m_{11}^2, m_{22}^2, m_s^2 and μ^2 and the quartic coupling terms λ_i, the cubic coupling terms κ, ζ and ξ, where we assume that all couplings are real. Since we are working within the conserving and scale invariant case we set m_{11}^2, m_{22}^2, m_s^2, μ^2, κ, $\xi = 0$. This further entails that there will be no CP violation as the model is in a CP-conserving case. We further impose $\mathbb{Z}_2$ symmetry on the singlet field and the Higgs doublet,

$$
H_1 \leftrightarrow H_1, \quad H_2 \leftrightarrow -H_2, \quad S \leftrightarrow -S,
\tag{2.5}
$$

to mitigate unwanted flavor-changing neutral currents (FCNCs) [19]. This changes the model to one forbidding the quadratic terms $H_1^\dagger H_2 + H_2^\dagger H_1$. This leads to the use of the following potential in this study:

$$
\begin{aligned}
V_{tree} = & \frac{\lambda_1}{2} \left(H_1^\dagger H_1 \right)^2 + \frac{\lambda_2}{2} \left(H_2^\dagger H_2 \right)^2 + \lambda_3 \left(H_1^\dagger H_1 \right) \left(H_2^\dagger H_2 \right) + \lambda_4 \left(H_1^\dagger H_2 \right) \left(H_2^\dagger H_1 \right) \\
& + \frac{\lambda_5}{2} \left[\left(H_1^\dagger H_2 \right)^2 + \left(H_2^\dagger H_1 \right)^2 \right] + \frac{\lambda_6}{8} S^4 + \frac{1}{2} \left[\lambda_7 H_1^\dagger H_1 + \lambda_8 H_2^\dagger H_2 \right] S^2.
\end{aligned}
\tag{2.6}
$$

To determine when the scalar potential V_{tree} stabilizes at a non-trivial minimum, the tadpole conditions [20] are applied. These conditions require the first derivatives of the potential with respect to each field to be zero at the minimum, ensuring vacuum stability. They are set up as a system of equations, where one solves for expressions of the coupling terms, in this case λ_6, λ_7, and λ_8. Due to the flat direction in the potential, this results in a massless scalar. This leads to the following specific tadpole conditions when minimizing Eq. (2.6):

$$
T_{\text{tree}}^1 = \left\langle \frac{\partial V_{\text{tree}}}{\partial \varphi_1^0} \right\rangle = \frac{1}{4} v_1 \left(2 v_1^2 \lambda_1 + 2 v_2^2 \lambda_{345} + v_s^2 \lambda_7 \right) = 0,
\tag{2.7}
$$

$$
T_{\text{tree}}^2 = \left\langle \frac{\partial V_{tree}}{\partial \varphi_2^0} \right\rangle = \frac{1}{4} v_2 (2 v_2^2 \lambda_2 + 2 v_1^2 \lambda_{345} + v_s^2 \lambda_8) = 0,
\tag{2.8}
$$

$$
T_{\text{tree}}^3 = \left\langle \frac{\partial V_{tree}}{\partial \varphi_s} \right\rangle = \frac{1}{8} v_s (v_s^2 \lambda_6 + 2 v_1^2 \lambda_7 + 2 v_2^2 \lambda_8) = 0,
\tag{2.9}
$$

where $\lambda_{345} = \lambda_3 + \lambda_4 + \lambda_5$, φ_1^0 and φ_2^0 are the CP-even Higgs states, and ϕ_s is the real singlet.

Subsequently, we use these tadpole conditions to solve for the squared mass matrix, constructed by taking the second derivative of the potential with respect to the field components as follows:

$$\mathbb{M}_{ij} = \left.\frac{\partial^2 V}{\partial\varphi_i \partial\varphi_j^\dagger}\right|_{\varphi=\langle\varphi\rangle} \qquad \text{for } i,j = 1,\ldots,7. \tag{2.10}$$

The 7×7 Hessian matrix, after applying the tadpole conditions, is organized into distinct 2×2 blocks, as well as one 3×3 block, along its diagonal. The order of these blocks is determined by the structure $\varphi_i = \{\phi_1^+, \phi_2^+, \varphi_1^0, \varphi_2^0, \varphi_s, a_1^0, a_2^0\}$, where ϕ_1^+ and ϕ_2^+ are complex terms. This arrangement clearly outlines the coupling terms and their relationships to the mass terms for various fields.

The first two 2×2 blocks and the final one are represented by the charged Higgs field $H^\pm$ and the CP odd field A respectively, and can both be diagonalized [11] by the following rotational matrix which coincides with the Higgs basis [[17],[14],[21]],

$$\begin{pmatrix} c_\beta & -s_\beta \\ s_\beta & c_\beta \end{pmatrix} \begin{pmatrix} -\frac{1}{2}v^2\lambda_{45}s_\beta^2 & \frac{1}{4}v^2\lambda_{45}s_{2\beta} \\ \frac{1}{4}v^2\lambda_{45}s_{2\beta} & -\frac{1}{2}v^2\lambda_{45}c_\beta^2 \end{pmatrix} \begin{pmatrix} c_\beta & s_\beta \\ -s_\beta & c_\beta \end{pmatrix} = \begin{pmatrix} 0 & 0 \\ 0 & M_{H^\pm}^2 \end{pmatrix}, \tag{2.11}$$

$$\begin{pmatrix} c_\beta & -s_\beta \\ s_\beta & c_\beta \end{pmatrix} \begin{pmatrix} -v^2\lambda_5 s_\beta^2 & v^2\lambda_5 c_\beta s_\beta \\ v^2\lambda_5 c_\beta s_\beta & -v^2\lambda_5 c_\beta^2 \end{pmatrix} \begin{pmatrix} c_\beta & s_\beta \\ -s_\beta & c_\beta \end{pmatrix} = \begin{pmatrix} 0 & 0 \\ 0 & M_A^2 \end{pmatrix}, \tag{2.12}$$

where $\lambda_{45} = \lambda_4 + \lambda_5$. This results in the charged mass $M_{H^\pm}^2 = -\frac{1}{2}v^2\lambda_{45}$ and the CP-odd mass $M_A^2 = -v^2\lambda_5$, which both match with Lee & Pilafstis work [11]. For both terms, the Goldstone bosons [15] $G^\pm$and G^0 become the longitudinal components of the gauge bosons $W^\pm$ and Z^0 and thereby acquiring mass.

What remains of the Hessian is a 3×3 matrix involving the CP-even mass terms that describe the mixing of the CP-even Higgs states $\varphi_{1,2}^0$ with the additional real singlet φ_s:

$$\begin{pmatrix} v_1^2\lambda_1 & v_1v_2\lambda_{345} & -\frac{v_1\left(v_1^2\lambda_1+v_2^2\lambda_{345}\right)}{v_s} \\ v_1v_2\lambda_{345} & v_2^2\lambda_2 & -\frac{v_2\left(v_2^2\lambda_2+v_1^2\lambda_{345}\right)}{v_s} \\ -\frac{v_1\left(v_1^2\lambda_1+v_2^2\lambda_{345}\right)}{v_s} & -\frac{v_2\left(v_2^2\lambda_2+v_1^2\lambda_{345}\right)}{v_s} & \frac{v_1^4\lambda_1+v_2^4\lambda_2+2v_1^2v_2^2\lambda_{345}}{v_s^2} \end{pmatrix}. \tag{2.13}$$

By diagonalizing the 3×3 matrix we obtain three physical mass eigenstates. The first, a Goldstone boson [13] and further we also identify two CP-even physical masses, $M_{h_2}^2$ and

$M^2_{h_3}$, defined in Appendix A. The Goldstone boson arises from the spontaneous breaking of classical scale symmetry due to a non-zero flat direction in the Higgs potential, resulting in a massless CP-even state typically called the scalon [11].

For practical calculations in what follows, we invert the parameter space of the model, $\lambda_{1,2,4,5}$ with respect to the tree level physical masses $M^{tree}_{H^\pm}$, M^{tree}_{A}, $M^{tree}_{h_2}$, $M^{tree}_{h_3}$, in order to perform numerical scans of the model.

2.3 One-loop radiative corrections to the mass spectrum

In the SI-2HDM, quantum loops involving gauge, Higgs self-couplings, and top-quark interactions break the classical scale symmetry. This necessitates computing the one-loop effective potential and determining the radiatively corrected CP-even Higgs boson masses and their mixing. Due to the additional CP-even mass eigenstate obtained in the 3×3 mass matrix at tree-level, the CW potential [12] must be extended to include the effects of the additional CP-even mass state:

$$\begin{aligned} V_{\text{eff}} = \frac{1}{64\pi^2}\Bigg(&\mu^4_{h_2}\left(\ln\frac{\mu^2_{h_2}}{Q^2}-\frac{3}{2}\right)+\mu^4_{h_3}\left(\ln\frac{\mu^2_{h_3}}{Q^2}-\frac{3}{2}\right) \\ &+\mu^4_{A}\left(\ln\frac{\mu^2_{A}}{Q^2}-\frac{3}{2}\right)+2\mu^4_{H^\pm}\left(\ln\frac{\mu^2_{H^\pm}}{Q^2}-\frac{3}{2}\right) \\ &+6\mu^4_{W}\left(\ln\frac{\mu^2_{W}}{Q^2}-\frac{5}{6}\right)+3\mu^4_{Z}\left(\ln\frac{\mu^2_{Z}}{Q^2}-\frac{5}{6}\right)-12\mu^4_{t}\left(\ln\frac{\mu^2_{t}}{Q^2}-1\right)\Bigg), \end{aligned} \tag{2.14}$$

where Q is the renormalization scale [13] and the background field-dependent masses squared are given by the matching to their tree level expressions as following:

$$\mu^2_A = -2\lambda_5(H_1^\dagger H_1 + H_2^\dagger H_2), \qquad \mu^2_{H^\pm} = -\lambda_{45}(H_1^\dagger H_1 + H_2^\dagger H_2), \tag{2.15}$$

$$\mu^2_Z = \frac{g^2}{2c^2_w}(H_1^\dagger H_1 + H_2^\dagger H_2), \qquad \mu^2_W = \frac{g^2}{2}(H_1^\dagger H_1 + H_2^\dagger H_2), \tag{2.16}$$

$$\mu^2_t = 2\frac{m^2_t}{v^2 c^2_\beta}(H_2^\dagger H_2), \tag{2.17}$$

while $\mu^2_{h_2}$ and $\mu^2_{h_3}$ are given in Appendix A.

The squared masses $\mu^2_{h_2}$, $\mu^2_{h_3}$, μ^2_A, and $\mu^2_{H^\pm}$ are defined in the CW potential [11] by combinations of the quartic couplings $\lambda_{1,2,3,4,5}$. These reflect the dynamics within the Higgs sector, influenced by the two Higgs doublets H_i and the singlet S. The field-dependent gauge boson masses squared, M^2_Z and M^2_W, are derived from the weak coupling g, the cosine of the Weinberg angle c^2_w, and the Higgs contributions. The field-dependent top quark mass squared, μ^2_t, is influenced by the mass of the top quark m^2_t, vevs, and c^2_β.

The renormalization scale is defined by using the GW scheme [13] so that $Q = \Lambda_{GW}$ where the relation for Λ_{GW} is:

$$\log \frac{\Lambda_{GW}}{v} = \left(\frac{\boldsymbol{A}}{2\boldsymbol{B}} + \frac{1}{4} \right),$$

where the values for $\boldsymbol{B}$ and $\boldsymbol{A}$ are defined as:

$$\boldsymbol{B} = \frac{1}{64\pi^2 v^4} \left(\sum_{j \in \Pi} \beta_j M_j^2 \right), \tag{2.18}$$

$$\boldsymbol{A} = \frac{1}{64\pi^2 v^4} \sum_{j \in \Pi} \beta_j \langle \mu_j^4 \rangle \left(\alpha_j + \log \left(\frac{\langle \mu_j^2 \rangle}{v^2} \right) \right), \tag{2.19}$$

where $\Pi = \{h_2, h_3, A, H^{\pm}, W, Z, t\}$ represents the set of particles considered in the model, which are directly related to the field-dependent mass components of V_{eff}. The constants β_j and α_j are specific coefficients for each particle j in the set Π, where β_j represents the numerical coefficient for each field-dependent mass term μ_j^2, while α_j accounts for an additional constant affecting the logarithmic terms.

To gain a clearer analytical understanding of the one-loop tadpole equations, we use Π to indicate how the derivative can be simplified to show the contributing components of V_{eff}, similar to the approach in [22]. We define the total derivative of the one-loop potential, where all components contribute, as V_{Π}. When all components except the top quark t are included, it is denoted as $V_{\Pi \setminus t}$. If only the components related to the field-dependent CP-even mass terms remain in the derivative, it is denoted as $V_{h_{2,3}}$. This is specifically the case when differentiating V_{eff} with respect to the singlet field.

$$\begin{aligned}
\left\langle \frac{\partial V_{\text{tot}}}{\partial \varphi_1^0} \right\rangle &= T^1_{\text{tree}} + \left\langle \frac{\partial V_{\text{eff}}}{\partial \varphi_1^0} \right\rangle = T^1_{\text{tree}} + \left\langle \frac{\partial V_{\Pi \setminus \{t\}}}{\partial \varphi_1^0} \right\rangle = 0, \\
\left\langle \frac{\partial V_{\text{tot}}}{\partial \varphi_2^0} \right\rangle &= T^2_{\text{tree}} + \left\langle \frac{\partial V_{\text{eff}}}{\partial \varphi_2^0} \right\rangle = T^2_{\text{tree}} + \left\langle \frac{\partial V_{\Pi}}{\partial \varphi_2^0} \right\rangle = 0, \\
\left\langle \frac{\partial V_{\text{tot}}}{\partial \varphi_s} \right\rangle &= T^3_{\text{tree}} + \left\langle \frac{\partial V_{\text{eff}}}{\partial \varphi_s} \right\rangle = T^3_{\text{tree}} + \left\langle \frac{\partial V_{\{h_{2,3}\}}}{\partial \varphi_s} \right\rangle = 0,
\end{aligned} \tag{2.20}$$

These tadpole equations of the total potential are used with eq. (2.10) to calculate the new mass matrix. Due to the complexity of the solutions a numerical analysis is performed to get the final results for the mass eigenstate values corresponding to the physical mass values by diagonalizing the matrix.

3 Numerical Analysis

The computational implementation is carried out using a custom Mathematica script, which systematically explores the random parameter space. The script operates by sequentially varying the parameters within defined ranges, ensuring that the entire process runs through multiple iterations to produce the final result. This comprehensive approach allows for a thorough analysis of the model's behavior under different conditions, as described in the following steps.

The objective of the numerical analysis of the SI-2HDM+S is to explore the implications of the model under various parameter settings. To this end, a setup is employed where a multitude of parameters are randomly varied within specified ranges. The parameters and their respective ranges are specifically listed as follows:

$$\begin{aligned} M_A^{tree}, M_{h_2}^{tree}, M_{h_3}^{tree}, M_{H^\pm}^{tree} &: 100 \text{ GeV} \leq M \leq 300 \text{ GeV}, \\ |\lambda_3| &< 1, \\ \tan\beta &: 1 \leq \tan\beta \leq 20, \\ v_s &: 50 \text{ GeV} \leq v_s \leq 500 \text{ GeV}, \\ v &: 246 \text{ GeV}. \end{aligned}$$

The analysis continues by defining the coupling constants λ_i in terms of the mass parameters, using the field-dependent masses for λ_1, λ_2, λ_4, and λ_5, as well as the minimization conditions of the total potential, eq. (2.20), to obtain the definitions for the couplings λ_6, λ_7, and λ_8. For each set of random parameters, the model's equations are solved to determine the eigenvalues of the mass matrix derived from the total loop-corrected potential by diagonalization.

We choose to consider the state corresponding to the smallest of these eigenvalues, M_{h_1}, following the GW scale, as a candidate for the SM-like Higgs boson under the assumption that it represents a light, potentially observable particle.

4 Numerical Results

A parameter limit of 115-135 GeV was set for the CP-even masses, and the first seven results within this range, along with the various output parameters obtained during the model scan, are presented below.

Table 1: Data showing M_{h_1}, M_{h_2}, M_{h_3}, M_A, tan β , v_s, $M_{h_2}^{tree}$, $M_{h_3}^{tree}$, $M_{H^\pm}^{tree}$, and λ_3 values.

M_{h_1}	M_{h_2}	M_{h_3}	M_A	$\mathbf{tan}\beta$	v_s	$M_{h_2}^{tree}$	$M_{h_3}^{tree}$	$M_{H^\pm}^{tree}$	λ_3
130	132	196	295	13.2	462	199	148	232	0.106
125	127	184	233	13.3	445	150	251	155	0.983
123	124	184	246	19.9	385	285	156	158	0.355
131	131	194	125	17.0	340	298	165	108	0.415
126	127	190	288	16.1	360	296	163	116	0.228
120	147	184	114	3.12	190	242	297	251	0.810
124	124	187	103	10.5	275	230	173	210	0.576

Before analyzing the table, we impose an ordering at the one-loop level for $M_{h_1} < M_{h_2} < M_{h_3}$, defining the lightest CP-even mass term as the Higgs boson. From our numerical results, we observe several distinct parameter traits, most notably that multiple results within the correct range for the Higgs boson can be found for the lightest CP-even mass. However, as seen in Table 1, the lightest and second lightest masses are very close in range, while the heaviest CP-even mass differs by a clear amount. This disparity could be attributed to several factors. These include the additional contributions from the real singlet field, which enhance the mass of the pseudo-Goldstone boson, the significant impact of radiative corrections in the SI-2HDM+S model on the mass generation process, and the redistribution of mass eigenvalues resulting from the mixing terms involving the singlet field and the CP-even neutral scalars.

Furthermore, looking at other parameters of Table 1 reveals that there is no specific range for λ_3 and tan β. For the other parameters, a graphical approach is taken to better observe their constraints visually. This is done by following the numerical analysis.

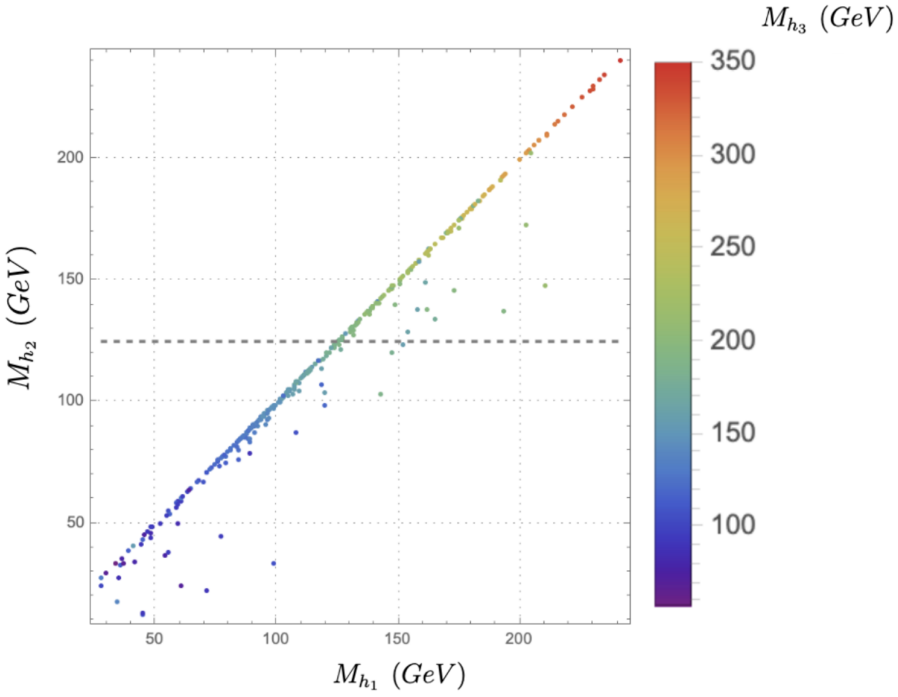

Figure 1: Comparison of the lightest eigenvalue M_{h_1} on the x-axis with M_{h_2} on the y-axis, with M_{h_3} represented as an additional parameter using a color scale.

Figure 1 demonstrates a strong linear relationship between M_{h_1} and M_{h_2}. Additionally, the color scale representing M_{h_3} indicates a similar linear relationship, though it is shifted slightly higher.

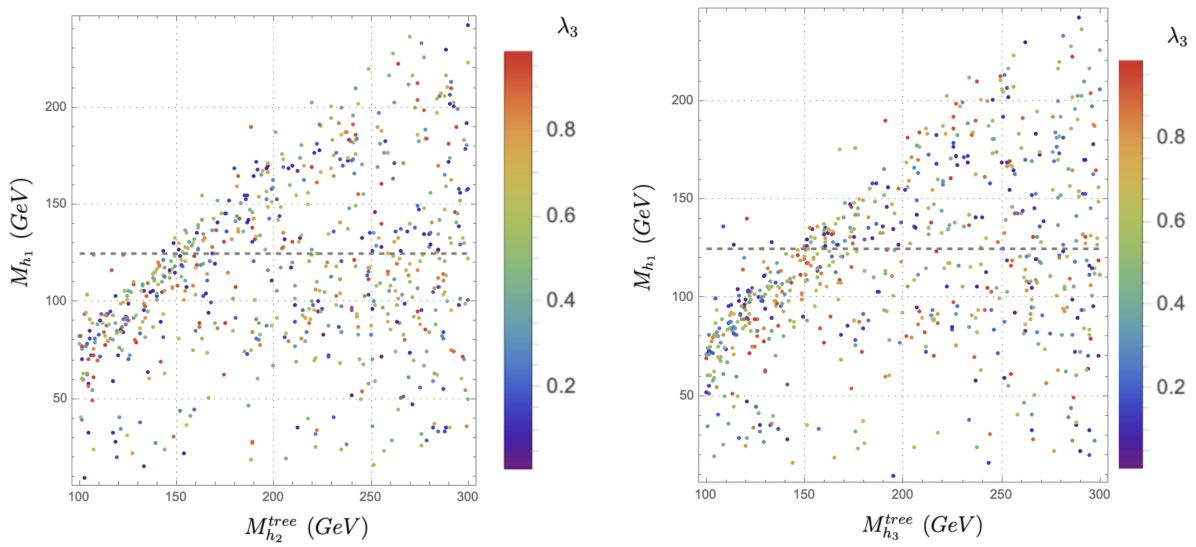

Figure 2: Comparison of the lightest eigenvalues M_{h_1} on the y-axis with $M_{h_2}^{tree}$ (left) and $M_{h_3}^{tree}$ (right) on the x-axis, with λ_3 represented as an additional parameter using a color scale.

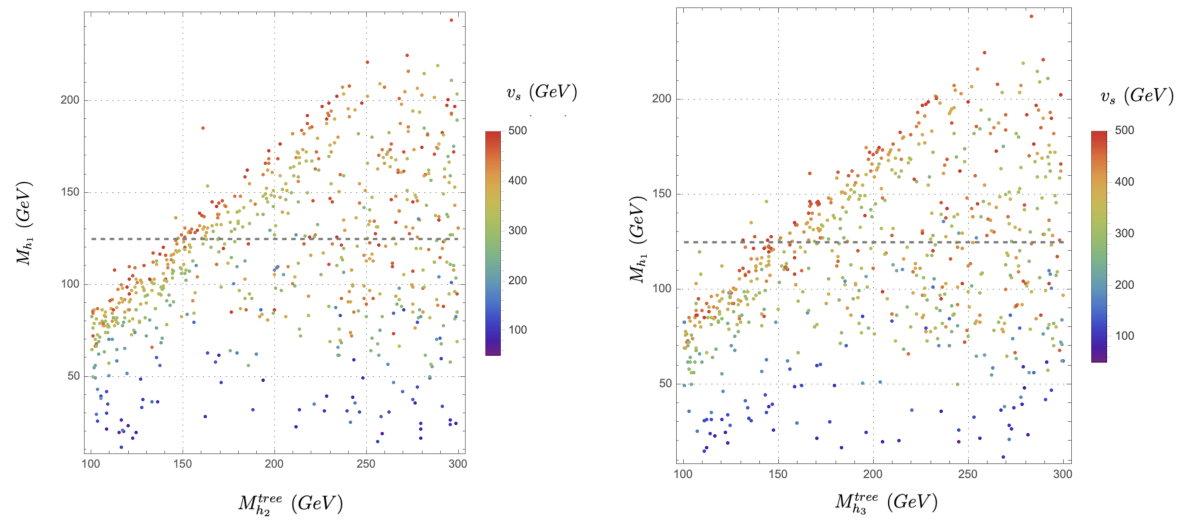

Figure 3: Comparison of the lightest eigenvalues M_{h_1} on the y-axis with $M_{h_2}^{tree}$ (left) and $M_{h_3}^{tree}$ (right) on the x-axis, with v_s represented as an additional parameter using a color scale.

Furthermore, both Figure 2 and Figure 3 reveal a relationship that serves as a boundary or guideline for the distribution of the lightest CP-even mass when comparing tree-level parameter CP-even masses with the lightest eigenvalues. These figures also provide a rough

estimate of the range of the tree-level mass $M_{h_3}^{tree}$, approximately 140-170 GeV, and for $M_{h_2}^{tree}$, around 150-180 GeV. This constrained parameter space could be due to the delicate balance required between the tree-level potential and the radiative corrections to achieve a stable vacuum and maintain consistency with experimental data.

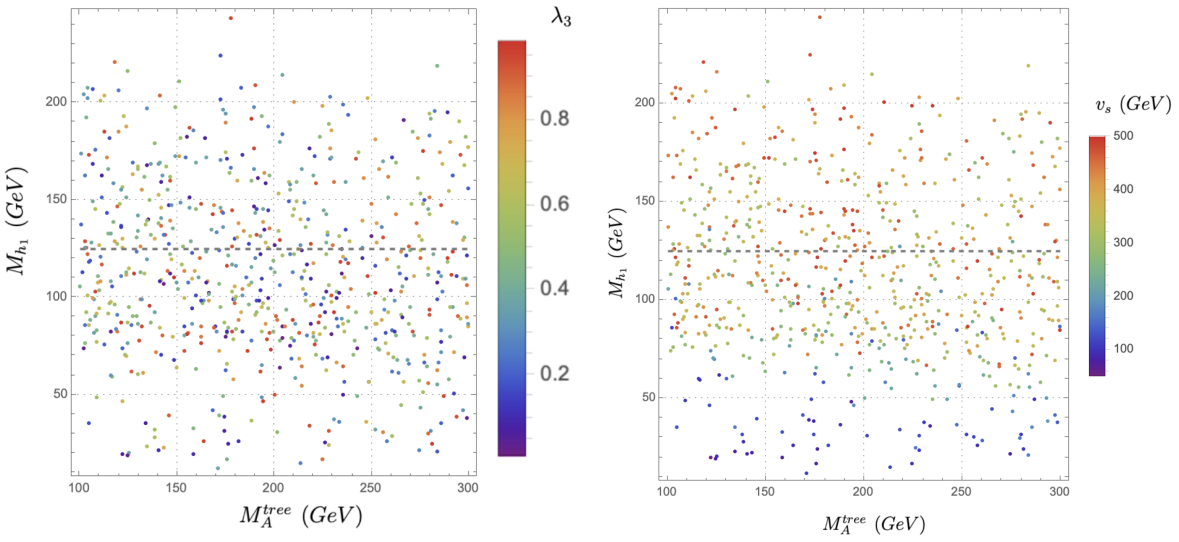

Figure 4: Comparison of the lightest eigenvalues M_{h_1} on the y-axis with M_A^{tree} on the x-axis, with λ_3 (left) and v_s (right) represented as additional parameters using a color scale.

For the parameter M_A^{tree}, there is no specific range when the lightest CP-even mass is around 125 GeV; instead, it can be any value, as shown in Fig. 4. However, what can be observed from this figure, as well as from Figure 3, is that v_s has a slight constraint, with its values lying around 300 GeV and slightly above.

Looking from a theoretical point of view and starting from the tree-level potential, we can observe significant differences between the SI-2HDM and SI-2HDM+S models. In the SI-2HDM+S model, the terms λ_6, λ_7, and λ_8 do not vanish as they would under a $\mathbb{Z}_2$ symmetry in the case of Lee & Pilaftsis [11]. This non-zero contribution from λ_6, λ_7, and λ_8 modifies the scalar potential and impacts the mixing terms, leading to a 3×3 mass matrix for the CP-even neutral scalars instead of a 2×2 matrix. Consequently, the SI-2HDM+S model predicts two additional CP-even neutral mass eigenstates compared to the SI-2HDM, which only predicts one.

Both models feature a Goldstone boson, which acquires mass through radiative corrections. At tree level, the SI-2HDM+S introduces an additional vev from the real singlet, affecting the mass terms of the CP-even neutral scalars. This additional mass term adjusts the CW potential and the GW renormalization scale, incorporating an extra term due to the singlet. As a result, the third tadpole condition in the CW potential, which typically vanishes in other models [22], retains both CP-even mass terms in the SI-2HDM+S.

It can further be stated that the tree-level masses and their one-loop corrections reveal that the couplings in the SI-2HDM+S model differ significantly from those in the SI-2HDM. Specifically, the introduction of the real singlet modifies the relationships among the couplings, leading to a richer phenomenology and different experimental signatures. The one-loop corrected masses show that the parameter space is tightly constrained to obtain a Higgs boson mass around 125 GeV.

5 Conclusion and Outlook

In conclusion, the SI-2HDM+S model introduces significant modifications to the scalar potential and mass spectrum compared to the SI-2HDM. The presence of an additional real singlet field and the non-zero λ_6, λ_7, and λ_8 terms lead to a lengthier mass matrix and an additional mass eigenstate. Our numerical analysis shows that the parameter space is tightly constrained to achieve a Higgs boson mass around 125 GeV.

The next natural steps to study the SI-2HDM+S model include a detailed investigation of the interactions between the proposed Higgs boson candidates and other particles, such as gauge bosons and fermions. Understanding these interactions is crucial as they may differ from those of the Higgs boson, providing further insights into the model's validity and potential experimental signatures. Additionally, a thorough analysis of the eigenstates of the mass matrix at the one-loop level should be conducted to determine why the degeneracy between the two lightest mass terms exists. This analysis should also identify which physical mass corresponds to each mass eigenstate, as experimentally this may result in the observation of only one mass, but this remains to be investigated.

Future research could also explore a broader range of areas. This includes reproducing the Higgs state and studying its constraints from collider data, and examining how these states behave in the early universe, particularly when considering thermal corrections. Such studies are essential for understanding the model's implications and ensuring its consistency with experimental and cosmological observations.

A Appendix

The following shows the calculated CP-even mass eigenstates M_{h_2} and M_{h_3} defined in terms of λ_i:

$$M_{h_2}^2 = \frac{v_s^3\left(v_1^2\lambda_1 + v_2^2\lambda_2\right) + v_s\left(v_1^4\lambda_1 + v_2^4\lambda_2 + 2v_1^2v_2^2\lambda_{345}\right)}{2v_s^3}$$

$$- \frac{\sqrt{-4v_1^2v_2^2v_s^4\left(v^2+v_s^2\right)\left(\lambda_1\lambda_2 - \lambda_{345}^2\right) + v_s^2\left(v_1^4\lambda_1 + v_2^2\left(v_2^2+v_s^2\right)\lambda_2 + v_1^2\left(v_s^2\lambda_1 + 2v_2^2\lambda_{345}\right)\right)^2}}{2v_s^3}$$

$$M_{h_3}^2 = \frac{v_s^3\left(v_1^2\lambda_1 + v_2^2\lambda_2\right) + v_s\left(v_1^4\lambda_1 + v_2^4\lambda_2 + 2v_1^2v_2^2\lambda_{345}\right)}{2v_s^3}$$
$$+\frac{\sqrt{-4v_1^2v_2^2v_s^4\left(v^2+v_s^2\right)\left(\lambda_1\lambda_2-\lambda_{345}^2\right)+v_s^2\left(v_1^4\lambda_1+v_2^2\left(v_2^2+v_s^2\right)\lambda_2+v_1^2\left(v_s^2\lambda_1+2v_2^2\lambda_{345}\right)\right)^2}}{2v_s^3}$$

The field dependent masses for $\mu_{h_2}^2$ and $\mu_{h_3}^2$ are as follows:

$$\mu_{h_2}^2 = (H_1^\dagger H_1)\lambda_1 + (H_2^\dagger H_2)\lambda_2 + \frac{2((H_1^\dagger H_1)^2\lambda_1 + (H_2^\dagger H_2)^2\lambda_2 + 2(H_1^\dagger H_1)(H_2^\dagger H_2)\lambda_{345})}{S^2}$$
$$- \frac{\sqrt{\left(-4(H_1^\dagger H_1)(H_2^\dagger H_2)S^2\left(2((H_1^\dagger H_1)+(H_2^\dagger H_2))+S^2\right)\left(\lambda_1\lambda_2-\lambda_{345}^2\right)+2(H_2^\dagger H_2)^2\lambda_2\right.}}{S^2}$$
$$\frac{\left.+2(H_1^\dagger H_1)\left((H_1^\dagger H_1)\lambda_1+2(H_2^\dagger H_2)\lambda_{345}\right)+\left((H_1^\dagger H_1)\lambda_1+(H_2^\dagger H_2)\lambda_2\right)S^2)^2\right.}}{S^2}$$

$$\mu_{h_3}^2 = (H_1^\dagger H_1)\lambda_1 + (H_2^\dagger H_2)\lambda_2 + \frac{2((H_1^\dagger H_1)^2\lambda_1 + (H_2^\dagger H_2)^2\lambda_2 + 2(H_1^\dagger H_1)(H_2^\dagger H_2)\lambda_{345})}{S^2}$$
$$+ \frac{\sqrt{\left(-4(H_1^\dagger H_1)(H_2^\dagger H_2)S^2\left(2((H_1^\dagger H_1)+(H_2^\dagger H_2))+S^2\right)\left(\lambda_1\lambda_2-\lambda_{345}^2\right)+2(H_2^\dagger H_2)^2\lambda_2\right.}}{S^2}$$
$$\frac{\left.+2(H_1^\dagger H_1)\left((H_1^\dagger H_1)\lambda_1+2(H_2^\dagger H_2)\lambda_{345}\right)+\left((H_1^\dagger H_1)\lambda_1+(H_2^\dagger H_2)\lambda_2\right)S^2)^2\right.}}{S^2}$$

Acknowledgements

I would like to express my sincere gratitude to my supervisor, Roman Pasechnik, for his guidance and support throughout the entire process. Additionally, I wish to extend my thanks to Johan Rathsman and Johan Bijnens for their review and constructive feedback.

References

[1] Steven Weinberg. A Model of Leptons. *Phys. Rev. Lett.*, 19:1264–1266, Nov 1967. DOI: 10.1103/PhysRevLett.19.1264.

[2] Steven Weinberg. Essay: Half a Century of the Standard Model. *Phys. Rev. Lett.*, 121:220001, Nov 2018. DOI: 10.1103/PhysRevLett.121.220001.

[3] G. et al. Aad. Observation of a new particle in the search for the Standard Model Higgs boson with the ATLAS detector at the LHC. *Physics Letters B*, 716(1):1–29, Sep 2012. DOI: 10.1016/j.physletb.2012.08.020.

[4] Peter W. Higgs. Broken symmetries and the masses of gauge bosons. *Phys. Rev. Lett.*, 13:508–509, Oct 1964. DOI: 10.1103/PhysRevLett.13.508.

[5] David E Morrissey and Michael J Ramsey-Musolf. Electroweak baryogenesis. *New Journal of Physics*, 14(12):125003, Dec 2012. DOI: 10.1088/1367-2630/14/12/125003.

[6] Gerald S. Guralnik. The history of the Guralnik, Hagen, and Kibble development of the theory of spontaneous symmetry breaking and gauge particles. *International Journal of Modern Physics A*, 24(14):2601–2627, Jun 2009. DOI: 10.1142/S0217751X09045431.

[7] Michael Dine and Alexander Kusenko. Origin of the matter-antimatter asymmetry. *Rev. Mod. Phys.*, 76:1–30, Dec 2003. DOI: 10.1103/RevModPhys.76.1.

[8] A. Arbey and F. Mahmoudi. Dark matter and the early universe: A review. *Progress in Particle and Nuclear Physics*, 119:103865, Jul 2021. DOI: 10.1016/j.ppnp.2021.103865.

[9] T. D. Lee. A theory of spontaneous t violation. *Phys. Rev. D*, 8:1226–1239, Aug 1973. DOI: 10.1103/PhysRevD.8.1226.

[10] Igor P. Ivanov. Building and testing models with extended higgs sectors. *Progress in Particle and Nuclear Physics*, 95:160–208, Jul 2017. DOI: 10.1016/j.ppnp.2017.03.001.

[11] J. S. Lee and A. Pilaftsis. Radiative Corrections to Scalar Masses and Mixing in a Scale Invariant Two Higgs Doublet Model. *Phys. Rev. D*, 86:035004, Aug 2012. arXiv: 1201.4891 [hep-ph].

[12] Sidney Coleman and Erick Weinberg. Radiative corrections as the origin of spontaneous symmetry breaking. *Phys. Rev. D*, 7:1888–1910, Mar 1973. DOI: 10.1103/PhysRevD.7.1888.

[13] E. Gildener and S. Weinberg. Symmetry Breaking and Scalar Bosons. *Phys. Rev. D*, 13:3333–3341, 1976. DOI: 10.1103/PhysRevD.13.3333.

[14] H. E. Haber and S. Davidsson. Basis-independent Methods for the Two-Higgs-Doublet Model. *Phys. Rev. D*, 72:035004, 2005. DOI: 10.1103/PhysRevD.72.035004.

[15] Jeffrey Goldstone, Abdus Salam, and Steven Weinberg. Broken symmetries. *Phys. Rev.*, 127:965–970, Aug 1962. DOI: 10.1103/PhysRev.127.965.

[16] R. L. Workman et al. Review of Particle Physics. *PTEP*, 2022:083C01, 2022. DOI: 10.1093/ptep/ptac097.

[17] Howard E. Haber and Deva O'Neil. Basis-independent methods for the two-higgs-doublet model. ii. the significance of tan . *Physical Review D*, 74(1), Jul 2006. DOI: 10.1103/PhysRevD.74.015018.

[18] A. Arhrib, R. Benbrik, M. EL Kacimi, L. Rahili, and S. Semlali. Extended higgs sector of 2HDM with real singlet facing LHC data. *The European Physical Journal C*, 80(1), Jan 2020. DOI: 10.1140/epjc/s10052-019-7472-2.

[19] Sheldon L. Glashow and Steven Weinberg. Natural conservation laws for neutral currents. *Phys. Rev. D*, 15:1958–1965, Apr 1977. DOI: 10.1103/PhysRevD.15.1958.

[20] Sidney Coleman and S. L. Glashow. Departures from the eightfold way: Theory of strong interaction symmetry breakdown. *Phys. Rev.*, 134:B671–B681, May 1964. DOI: 10.1103/PhysRev.134.B671.

[21] G.C. Branco, P.M. Ferreira, L. Lavoura, M.N. Rebelo, Marc Sher, and João P. Silva. Theory and phenomenology of two-higgs-doublet models. *Physics Reports*, 516(1–2): 1–102, Jul 2012. DOI: 10.1016/j.physrep.2012.02.002.

[22] Jimmy Gunnarsson. A Study of Spontaneous CP Violation in the Scale Invariant 2HDM, 2022. URL `http://lup.lub.lu.se/student-papers/record/9095343`.